Res. **289**, 375 (1983); J. M. Candy *et al.*, *J. Neurol. Sci.* **54**, 277 (1983).

7. G. E. Gibson, C. Peterson, D. J. Jenden, *Science* **213**, 674 (1981); R. Strong *et al.*, *Neurobiol. Aging* **1**, 59 (1980); K. A. Sherman *et al.*, *ibid.* **2**, 99 (1981); N. R. Sims *et al.*, *J. Neurochem.* **38**, 488 (1982).
8. S. B. Dunnett *et al.*, *Brain Res.* **251**, 335 (1982).
9. W. C. Low *et al.*, *Nature (London)* **300**, 260 (1982).
10. R. G. M. Morris, P. Garrand, J. W. P. Rawlins, J. O'Keefe, *ibid.* **297**, 681 (1982); R. G. M. Morris, *Learn. Motiv.* **12**, 236 (1981). The test apparatus was a large circular pool (140 cm in diameter by 45 cm high) filled with water to a depth of 30 cm. The water was made opaque by the addition of approximately ½ liter of dried milk powder and thermostatically maintained at 26° ± 1°C. An 11 by 11 cm transparent platform 29 cm high was placed in a fixed location in the tank, 1 cm below the water surface. Many extramaze cues surrounded the maze and were available for the rats to use in locating the escape platform. The experimenter conducting the behavioral tests was always unaware of the group assignments of the animals. On each trial, the rat was placed in the water close to and facing the wall of the pool in one of four equally spaced locations. The rat was allowed to swim freely around the pool until it found the platform, onto which it promptly climbed to escape from the water. If a rat failed to locate the platform within 120 seconds, it was then placed there by the experimenter. The intertrial interval was 60 seconds, during which the rat remained on the platform. Each rat received eight trials per day for 5 days. On the first 36 trials the platform remained in a constant location equidistant from the center and the edge of the pool, in the center of the fourth quadrant. On each trial two measures were recorded: (i) the latency to escape onto the platform, measured by a stopwatch; and (ii) the length of the swim path, measured by observation and tracing the swim path onto a "Hipad" analog-digital converter attached to an ABC80 microprocessor. On trial 5 of day 5 the platform was removed from the pool, and the total swim distance in each quadrant was measured over 120 seconds.
11. F. H. Gage, S. B. Dunnett, A. Björklund, *Neurobiol. Aging*, in press.
12. R. H. Schmidt, A. Björklund, U. Stenevi, *Brain Res.* **218**, 347 (1981).
13. A. Björklund *et al.*, *Acta Physiol. Scand. Suppl.* **522**, 1 (1983).
14. Septal cell suspensions were prepared from the developing basal forebrain dissected from E14-E16 donor rat fetuses (crown-rump length, 13 to 15 mm) of the same inbred strain. Although designated "septal," the dissected tissue contained the precursor cells of the entire septal-diagonal band complex and probably also the nucleus basalis (*13*). The tissue from 10 to 12 fetuses was collected in 0.6 percent glucose-saline in room temperature, incubated in 0.6 percent glucose–0.1 percent trypsin-saline for 20 minutes at 37°C, washed, and mechanically dissociated in 0.1 ml of glucose-saline to form a milky cell suspension. Aged rats were anesthetized with a ketamine-xylazine mixture [10 mg/kg Ketalar (Parke-Davis) and 5 mg/kg Rompun (Hoechst); intramuscular or intraperitoneal injections] and received stereotaxic injections of three 3-μl deposits of the cell suspension into the hippocampus on each side. Injection coordinates were: 4.5 mm anterior (A) to the interaural line, ±3.5 mm lateral (L) to the midline; and 3.0 mm ventral (V) to the dura; A = +3.0 mm, L = ±3.7 mm, V = 3.7 mm; and A = +3.0 mm, L = ±4.8 mm, V = 5.7 mm, with the incisor bar set at the level of the interaural line.
15. L. L. Butcher and L. Bijezikjian, *Eur. J. Pharmacol.* **34**, 115 (1975); S. A. Geneser-Jensen and T. Blackstad, *Z. Zellforsch.* **114**, 460 (1971).
16. F. H. Gage, S. B. Dunnett, U. Stenevi, A. Björklund, *Science* **221**,966 (1983).
17. A. Björklund *et al.*, *Brain Res.* **199**, 307 (1980); R. H. Schmidt *et al.*, *Acta Physiol. Scand. Suppl.* **522**, 19 (1983); A. Björklund *et al.*, *ibid.*, p. 59.
18. R. J. Sutherland, I. Q. Whishaw, J. C. Regehr, *J. Comp. Physiol. Psychol.* **96**, 563 (1982); F. H. Gage *et al.*, *Neurosci. Abstr.* **13**, 1979 (1983); R. T. Bartus, R. L. Dean, B. Beer, *Neurobiol. Aging* **1**, 145 (1980); R. T. Bartus *et al.*, *ibid.* **2**, 105 (1981).

19. We thank U. Jarl, C. Jönsson, and Y. Jönsson for expert technical assistance. Supported by grants from the National Institutes of Aging (AG 03766) and the Swedish Medical Research Council (04X-3874).

13 February 1984; accepted 17 May 1984

Interaction Between Perceived Self-Motion and Object-Motion Impairs Vehicle Guidance

Abstract. *When one is riding in a vehicle, perceptual thresholds for motion of objects are significantly elevated above those determined under corresponding but simulated conditions in the laboratory without concurrent self-motion perception. Authorities on road traffic accidents should thus consider an additional perceptual time of at least 300 milliseconds for detecting critical changes in headway beyond the usual reaction time. Detection times thus corrected consequently lead to an alteration of our conception of safe intervehicle distances in a convoy. This elevation of thresholds for object-motion during self-motion, with its consequences for visual control of vehicle guidance, can be seen as a disadvantageous side effect of an otherwise beneficial space-constancy mechanism, which provides us with a stable world during locomotion.*

Under laboratory conditions thresholds for detecting object-motion are traditionally determined with the subject's head fixed by a biteboard. Under natural environmental conditions, however, a person moves freely with the twofold perceptual task of controlling self-motion and perceiving object-motion simultaneously. The incidental observation that one has considerable difficulties seeing the treetops moving in the wind while driving a vehicle led us to a systematic study of egocentric object-motion perception during concurrent self-motion. In a series of laboratory experiments we demonstrated significantly increased thresholds of object-motion perception during simultaneous self-motion perception under various stimulus conditions.

Active head oscillations about the vertical *z*-axis (amplitude, ±20°) raised the detection thresholds for object-motion (with a 1° target, $\dot{\varphi}$ = 5 deg/sec) with increasing frequency of the sinusoidal head movements (0, 0.5, 1.0, and 1.5 Hz) up to a factor of 3 (1.5 Hz) above that measured when the head was stationary (0 Hz). These elevated thresholds are not due to a retinal slip of the fixated target, because stabilization of the retinal image was complete for ±20° rotatory head movements up to a frequency of 1.5 Hz (*1*).

Passive lateral triangular head movements (amplitude, ±60°) with the vestibulo-ocular reflex suppressed by fixation of a head-coupled target result in a doubling of the thresholds for object-motion detection with head movements at 60° per second angular velocity (*2, 3*).

That real self-motion is not the essential stimulus for suppressed object-motion perception was demonstrated with objectively stationary subjects for whom apparent self-motion was visually induced by full-field optokinetic stimulation. Elevated object-motion thresholds were linked to the sensation of self-motion, as evidenced by comparison with small-field pattern stimulation, which did not induce apparent self-motion (*4, 5*).

On the basis of these laboratory data we hypothesized that while a person is riding in a vehicle, thresholds for the detection of changes in headway should be elevated because object-motion thresholds are elevated during self-motion. We tested our hypothesis with a field study (vehicle guidance under natural conditions) and a corresponding simulation in the laboratory, in which a

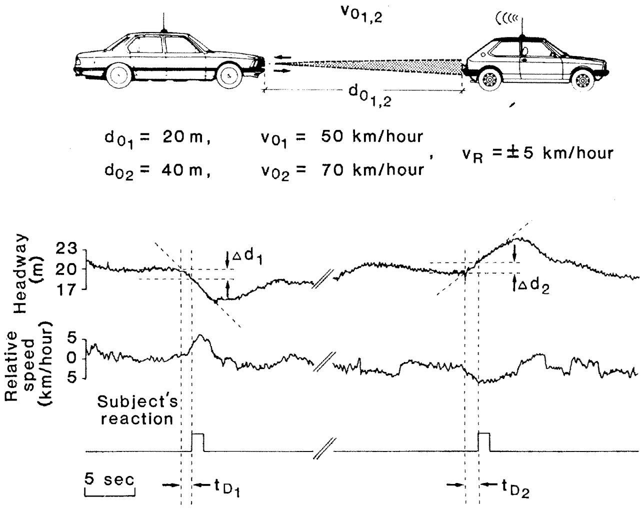

Fig. 1. Perception of changes in headway determined under real road conditions, at different absolute speeds ($v_{o_{1,2}}$) and distances ($d_{o_{1,2}}$). The intercar distance (headway) as well as relative speed (v_R) and subject's reaction latency (t_D) were recorded simultaneously.

stationary surround eliminated the perception of self-motion.

A motorway 4 km long and not yet open to public traffic was used for the field study. One of our two cars (BMW 728) was equipped with a distance radar—a bistatic pulse Doppler (35.4 GHz)—covering a range of 120 m and with a resolution of 0.5 m (Fig. 1). The second, leading car (Volkswagen Polo) served as the visual object, of which the headway was to be controlled by the driver of the BMW. Both cars were driven with headway distances d_{o_1} and d_{o_2} of 20 and 40 m with absolute speeds v_{o_1} and v_{o_2} of 50 and 70 km/hour. The subjects who drove the trailing car were required to detect changes in headway caused by a sudden relative velocity change v_R of about ± 5 km/hour of the leading car (which had no brake lights), resulting in a linearly increasing or decreasing change in distance between the two cars.

Relatively long reaction times were found for the visual detection of changes in headway with an average of 1.14 seconds for d_{o_1} of 20 m and v_{o_1} of 50 km/hour and 1.70 seconds for d_{o_2} of 40 m and v_{o_2} of 70 km/hour. Although less time was required to detect an approaching object than a receding one, this difference was not statistically significant.

Since the absolute speeds of 50 and 70 km/hour are well above the saturation level for linear vection (1 m/sec), we did not find different detection times under these two conditions (*6*). However, the times to detect changes in headway were significantly lower for the shorter distance (20 m) for both 50 km/hour [analysis of covariance: $F(1, 10) = 10.15$, $P < 0.003$] and 70 km/hour [$F(1, 9) = 5.35$, $P < 0.03$].

To evaluate our hypothesis that self-motion or visually induced self-motion perception considerably elevates object-motion detection thresholds under actual road conditions, we conducted a laboratory experiment in which the observed vehicle was simulated with an expanding or contracting visual array in the absence of the visual flow field present in the field study.

An approximation of the perceptually effective area of the rear of the leading car was simulated by an ellipse of equivalent retinal size that was electronically generated by two phase-displaced sine waves and an oscilloscope operating in the *x,y* mode. The image of the ellipse was transmitted by a television camera to a 50-cm monitor positioned 3.65 m in front of the subject. Headway changes were simulated by adjusting the retinal ellipse area with a triangle-wave generator; a linearized controllable resistor adjusted the retinal change in ellipse area in accordance with that of the real road conditions. This change in ellipse area was equivalent to that of an ellipse of fixed area moving in depth (sagittal plane) with a relative velocity of 1, 2, 4, or 6 km/hour. An increase in area simulated a headway reduction, and a decrease, a headway increase.

The times to detect changes in headway (Fig. 2) were significantly higher for the actual road condition (influence of the visual flow field) than for the corresponding simulation with a static visual array (in which mean detection times

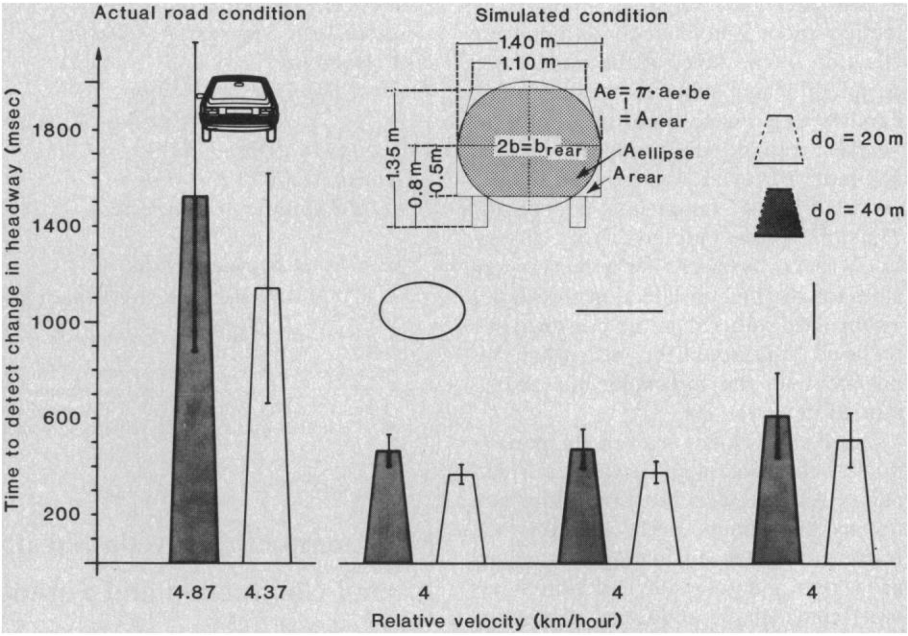

Fig. 2. Thresholds for the perception of changes in headway at distances of 20 and 40 m under real and simulated conditions without concurrent self-motion. Under static conditions in the laboratory there was no difference between the detection of a gradual change in area of the ellipse and a horizontal bar with the same but one-dimensional movement. Detection times, however, significantly increased ($\alpha < 0.05$) if object-movement occurred in corresponding but vertical dimensions only (vertical bar).

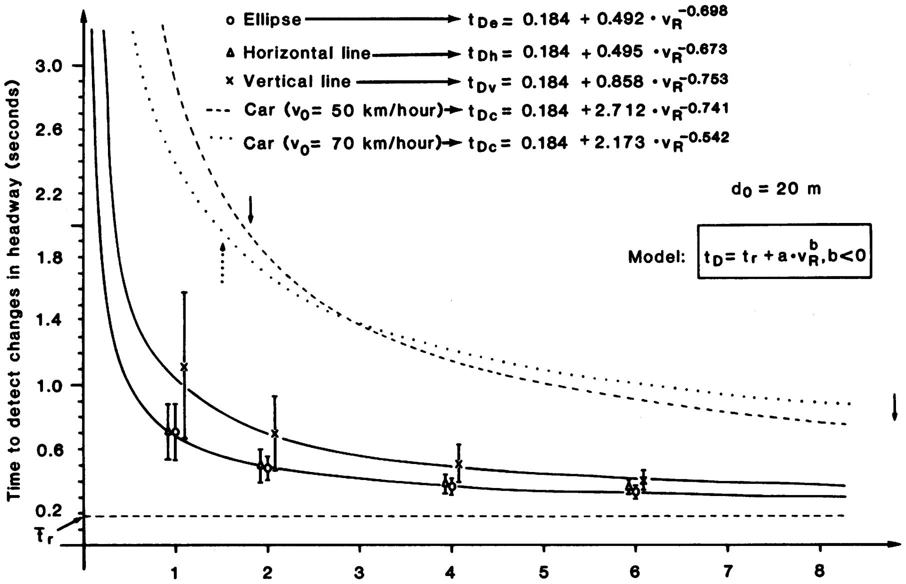

Fig. 3. Functions relating relative speed v_R (observer-object) and the time t_D to detect changes in area (○) or length (△, x) under static laboratory conditions (——) and under real road conditions for absolute speeds of 50 (- - - -) and 70 (· · · · ·) km/hour. The range of measured data (car experiment) is indicated by arrows. The dashed line $\bar{t}_r$ (184 msec) indicates "pure" reaction time for a suprathreshold stimulus independent of v_R; t_D is perception time plus "pure" reaction time.

were 332 msec for v_R of 6 km/hour and 709 msec for v_R of 1 km/hour at a simulated distance of 20 m). Curves fitted to the data (*7*) of both the field and laboratory experiments show for the overlapping range of relative velocities between about 2 and 6 km/hour a mean elevation factor of 3.27 ± 0.50 (range, 2.18 to 4.01) for the times to detect changes in headway under field conditions (Fig. 3).

The thresholds for object-motion detection under simulated conditions were elevated to the level of the vehicle experiment when subjects were simultaneously exposed to an artificial moving visual surround, which induces apparent self-motion, even though the ellipse characteristics remained unchanged. Thus, it is the perception of self-motion—real or apparent—which is responsible for the higher detection thresholds on the road rather than the presence of a textured background per se, which has no effect on the thresholds for object-motion detection (*8*).

During movement in a vehicle, perception of the motion of an object is impaired relative to perception under stationary conditions. Authorities on road traffic accidents evaluating perceptual processes and tolerable reaction times must consider the additional perceptual latencies involved in detecting changes in headway. Typically only the time span between the subjective perception of a critical traffic situation and the initiation of the braking maneuver is considered. Our data, however, also indicate a delay between the onset of the so-called objective stimulus situation (here, the very beginning of the change in headway) and the perceptibility of this event. This delay increases the total reaction time by at least 300 msec (d_o = 20 m, v_R = 19 km/hour, increasing with distance). Fifty percent of auto accidents involving rear end collisions occur with a relative velocity between the involved vehicles of only 19 km/hour (*9*). This interval is further increased by at least 250 msec if a saccadic change of gaze becomes necessary to fixate the potential obstacle (*10*). If a correction saccade is necessary an additional 130 msec is required (*11*).

As a consequence, drivers—particularly during high-density traffic flow—should not rely solely on their movement perception but rather should evaluate the flashing of the brake lights of the vehicle ahead as a trigger for an immediate brake response to minimize their reaction times. Additional brake lights at eye level are recommended to partially reduce these times (*12*). The subsequent control of braking force should be guided by the perception of the change in headway. The estimates of safe following distances should be corrected by taking into account the additional 300 msec required for perception of headway change. This duration must be added to the hitherto acceptable range of reaction times which varies between 0.6 and 1.0 seconds.

THOMAS PROBST
SIEGBERT KRAFCZYK
THOMAS BRANDT
Neurological Clinic Klinikum Grosshadern, University of Munich, 8000 Munich, Federal Republic of Germany
EUGENE R. WIST
Department of Psychology, University of Konstanz, 7750 Konstanz, Federal Republic of Germany

References and Notes

1. E. R. Wist, T. Brandt, S. Krafczyk, *Brain* **106**, 153 (1983).
2. T. Probst and E. R. Wist, *Perception* **11**, A33 (1982).
3. Adequate object-motion perception is also affected by smooth pursuit eye movements as demonstrated by Wertheim [*Acta Psychologica* **48**, 97 (1981)], who asked his subjects to detect the motion of a patterned visual field (background) during concurrent visual tracking of a single object projected onto the moving background.
4. Optokinetic full-field pattern motion induces, after a latency of several seconds, an apparent self-motion opposite in direction to pattern motion, indistinguishable from real self-motion, which is the result of a visual-vestibular convergence [J. Dichgans and T. Brandt, *Handbook of Sensory Physiology*, vol. 8, *Perception*, R. Held, H. W. Leibowitz, H.-L. Teuber, Eds. (Springer, Berlin, 1978), pp. 755–804].
5. D. Degner and T. Brandt, *Pflügers Arch.* **389** (Suppl.) R30, 118 (1981).
6. Linear vection is defined as a perception of linear self-motion induced by a moving visual scene (railway illusion) with a saturation level between 0.8 and 1.0 m/sec [A. Berthoz and J. Droulez, *Tutorials on Motion Perception*, A. H. Wertheim, W. A. Wagenaar, H. W. Leibowitz, Eds. (Plenum, New York, 1982), pp. 157–199.
7. Calculated with SAS (Statistical Analysis System, IBM 370/168 os, Nuclear Research Facility, Jülich, Federal Republic of Germany): nonlinear least-squares grid search.
8. L. O. Harvey and J. A. Michon, *J. Exp. Psychol.* **103**, 317 (1974).
9. A Study by German Motor Traffic Insurers on 28,936 Car Crashes with Passenger Injury [German Association of Third-Party Liability, Accident and Motor Traffic Insurers (HUK-Verband), Hamburg, 1975].
10. T. Uemura, Y. Arai, C. Shimazaki, *Acta Otolaryngol.* **90**, 191 (1980).
11. W. Becker and A. F. Fuchs, *Vision Res.* **9**, 1247 (1969).
12. IIHS Status Report **18**(15), 1 (1983).

10 November 1983; accepted 3 May 1984

Measurement of Myelin Sheath Resistances: Implications for Axonal Conduction and Pathophysiology

Abstract. *As commonly understood, the myelin sheath of axons insulates the internodal axolemma and essentially restricts transmembrane currents to nodal regions. However, recordings obtained from within the myelin sheath showed that its apparent resistance to current generated by action potentials is similar in magnitude to that of the internodal axolemma. This suggests that the sheath does not appreciably limit transmembrane current flow, presumably because there is a longitudinal shunt under the myelin and through the paranodal region. Thus, in some demyelinating diseases and other axonopathies, the safety factor for impulse conduction may be lowered by a loosening or a reduction in the number of paranodal axoglial junctions.*

Our present concepts of impulse conduction in myelinated axons developed from experiments (*1*) that demonstrated the insulating properties of myelin. In particular, the specific radial resistance of the internode was found to be high; its specific capacitance was low; and large inward and outward transmembrane ionic currents were observed only at the nodes. The membrane parameters derived from these studies have since been used in all computer models of impulse propagation along myelinated axons (*2–5*). Since it was not possible to distinguish the biophysical parameters of the two different internodal membranes, the sheath's radial resistance in these models has been assumed to be $2M$ (M being the number of myelin lamellae) times that of the internodal axonal membrane. These models have confirmed results of physiological studies of structure-function relationships (*3*) and have been used to predict the impulse conduction safety factor under conditions of demyelination (*4*, *5*). However, the data we report here, together with results obtained by others, indicate that the electrophysiological parameters of the internodal axolemma and its sheath, and the type of cable structure used to represent a myelinated axon, need to be reconsidered.

The morphological correlates of electrophysiologically localized active sites along the goldfish Mauthner axon were investigated (*6*). Except for its lack of typical nodal gaps, the structure-function relationships of the Mauthner axon and its myelin sheath were indistinguishable from those of other central and peripheral nervous system myelinated axons. In these experiments, intrasheath injections of Lucifer yellow or horseradish peroxidase from glass microelectrodes were used to determine the structure of the oligodendrocytes ensheathing